Korean J. Chem. Eng., **30**(9), 1797-1803 (2013)
DOI: 10.1007/s11814-013-0115-7

Co-precipitation of loperamide hydrochloride and polyethylene glycol using aerosol solvent extraction system

Edward Widjojokusumo*,, Bambang Veriansyah**, Yong-Suk Youn*, Youn-Woo Lee*,†, and Raymond Rubianto Tjandrawinata**,†**

*School of Chemical and Biological Engineering and Institute of Chemical Processes, Seoul National University, 1, Gwanak-ro, Gwanak-gu, Seoul 151-744, Korea
**Nanotechnology Research Laboratory, Advance Technology Development, Dexa Laboratories of Biomolecular Sciences (DLBS), PT Dexa Medica, Jl. Industri Selatan V, Blok PP no. 7, Kawasan Industri Jababeka 2 Cikarang, Bekasi 17550, Indonesia
(*Received 19 February 2013 • accepted 1 July 2013*)

Abstract−The co-precipitation of loperamide hydrochloride (LPM) and polyethylene glycol (PEG) using aerosol solvent extraction system (ASES) was examined. Scanning electron microscopy - energy dispersive X-ray spectroscopy (SEM-EDS) analysis showed that the co-precipitation was achieved in various LPM-PEG mass ratios with changes in its morphology. In 10-50% PEG mass ratios, angular-shaped particles were formed, whereas in 65-90% PEG mass ratios, irregular-shaped particles were formed. X-ray diffraction (XRD) analysis of the co-precipitates revealed that the LPM retained amorphous structure, while, on the other hand, the PEG retained crystalline structure. Fourier transform infrared (FT-IR) spectra indicated carbonyl function group of LPM and ether function group of PEG appeared in the co-precipitates. Results of a dissolution test showed that the co-precipitates of LPM-PEG had higher dissolution rate compared to that of the raw material and processed LPM with ASES. Taken together, the co-precipitation of LPM-PEG was achieved using ASES and higher in its dissolution rate.

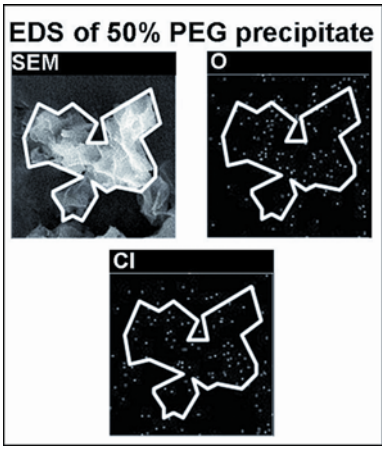

EDS of 50% PEG precipitate showed that chlorine map (indicate LPM) and oxygen map (indicate PEG) are co-precipitated

Key words: Loperamide Hydrochloride, Polyethylene Glycol, Co-precipitation, ASES

INTRODUCTION

Many newly developed drugs that have been approved are Biopharmaceutics Classification System (BCS) class II drugs for their low water solubility and high permeability properties. Physical characteristics of BCS class II drugs have limitation in their dissolution rate which is correlated with bioavailability of the drugs in the body [1]. Therefore, formulating and modifying physical characteristics to enhance the *in vitro* dissolution rate has become a primary issue in the pharmaceutical industry [2].

Co-precipitation of BCS class II drugs and hydrophilic polymers, generally known as solid dispersion or solid solution, has shown promising results to enhance the dissolution rate. The dissolution enhancement of solid dispersion can be achieved through reduction of particle size, absence of drug crystal aggregation or agglomeration, solubilization effect of polymer, excellent wettability and dispersibility of the drug, and partial conversion of the drug into amorphous form [2-4]. Commonly used methods in solid dispersion are solvent evaporation and fusion. However, industrial application of those methods is limited due to poor reproducibility, difficulty in removing of residual organic solvent, drug decomposition at high temper-

†To whom correspondence should be addressed.
E-mail: ywlee@snu.ac.kr, raymond@dexa-medica.com

ature, problem in product grinding, and physical instability of co-precipitates during storage [4,5].

Supercritical and subcritical carbon dioxide (Tc=304.18 K and Pc=7.38 MPa) has widely been used as solvent or antisolvent for preparation of nanoparticles or submicron particles in recent years. It has the ability to control mass transfer properties of carbon dioxide (CO_2), which is important for particle formation in the aerosol solvent extraction system (ASES), a process which uses CO_2 as an antisolvent. Co-precipitation of solute in ASES is caused by a decreased solvent power of organic solvent as a result of CO_2 diffusion to organic solvent, which leads to volume expansion or solvent evaporation [6]. ASES process can be applied for single [7-9] or multi compound(s) to produce inclusion co-precipitates [10,11], microspheres and microencapsulation [12], and other co-precipitates [5,13-17]. In this study, we examined co-precipitation of loperamide hydrochloride and polyethylene glycol using ASES. Loperamide hydrochloride (LPM) is an anti-diarrhea drug that is classified in BCS class II. Polyethylene glycol (PEG) is a hydrophilic polymer commonly used for co-precipitation due to its good solubility in various solvents and especially its low toxicity level [3,14]. The effect of mass ratios on the co-precipitates morphology and structure will be described as determined by scanning electron microscopy (SEM) and X-ray diffraction (XRD). The surface of the co-precipitates was characterized using Fourier transform infrared (FT-IR) and the LPM content of the co-precipitates was quantified with high performance liquid chromatography (HPLC).

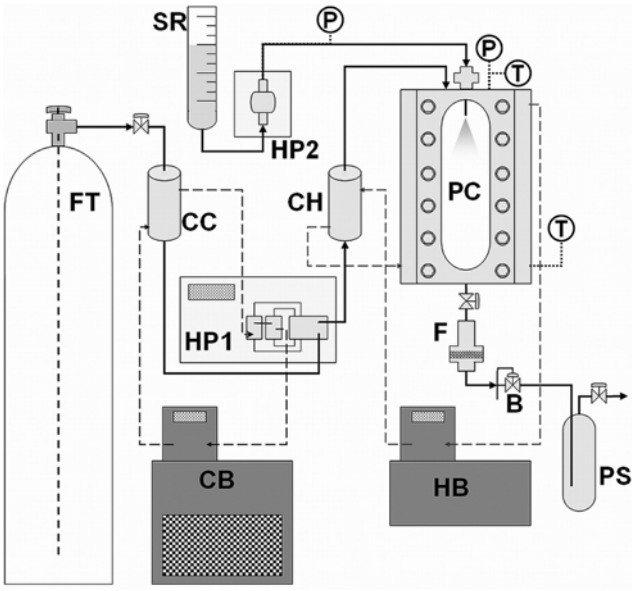

Fig. 1. Schematic diagram of a custom-built ASES apparatus. B, back pressure regulator; F, filter; CB, cooling bath; CC, precooler; CH, preheater; FT, CO_2 cylinder; HB, heating bath; HP1, high-pressure pump for the solution; HP2, high-pressure for carbon dioxide; PC, precipitation chamber; PS, phase separator; SR, solution reservoir.

EXPERIMENTAL METHODS

1. Materials

Loperamide hydrochloride (LPM) was purchased from Cychem Co (Danjinggo, South Korea) with particle size 34.93±31.88 μm. Polyethylene glycol (PEG, with an average M_w of 6,000) and triethylamine hydrochloride (HPLC grade) were purchased from Fluka Analytical (Buchs, Switzerland). The HPLC grade of methylene chloride (MC), methanol and acetonitrile was obtained from J.T. Baker, Inc. (New Jersey, USA). Hydrochloric acid (purity of 37%) was obtained from Sigma-Aldrich, Co. (Missouri, USA). High purity of carbon dioxide 99% (CO_2) was purchased from Korea Industrial Gases Ltd. (Seoul, Korea). 0.5 μm polytetrafluoroethylene (PTFE) membrane filter was obtained from Millipore (Massachusetts, USA).

2. Apparatus and Procedure

Co-precipitation was conducted using a custom-built aerosol solvent extraction system apparatus (ASES). A schematic diagram of the ASES system is shown in Fig. 1. The solution reservoir (SR) was a modified 110 mL size Pyrex burette. High-pressure pump for solution (HP1) was Milton Roy Mini Pump (Milton Roy, PA, USA) and for carbon dioxide (HP2) was HKS-300 digital pump (Hanyang Accuracy, Seoul, Korea). The precipitation chamber (PC) was made of stainless steel 316 (SS316) with 75 ml internal volume and water jacket to control the temperature of the precipitator. To observe the process of particle formation, a pair of glass windows was installed in front and back side of the PC. A stainless steel capillary tube with internal diameter of 0.0254 cm used as a nozzle was allocated on top of the PC. The carbon dioxide precooler (CC) and preheater (CH) were a shell and tube type. The inner tube was a 0.6 m in length and 3.175 mm outside diameter that made of SS316. The shell was made from SS316 with 0.11 m in diameter and 0.25 m in length. The co-precipitates were filtered with 0.5 μm polytetrafluoroethylene (PTFE) membrane filter (F). Pressure of the PC was controlled using a model 26-1721-24 back pressure regulator (B), manufactured by Tescom, Co. (MN, USA).

Prior to each experiment, the temperature of the PC was set to an experimental temperature of 288 K, and CO_2 was cooled before

Table 1. The experimental condition and particle size of the LPM-PEG co-precipitate

PEG mass ratio (%)	T (K)	P (MPa)	Concentration (mg/mL)	Flow rate (mL/min)	Particle size (mean±SD μm)
10	288	15	11.11	0.53	1.74±1.31
20	288	15	12.5	0.53	2.47±1.44
35	288	15	15.38	0.53	3.39±1.76
50	288	15	20	0.53	3.13±1.78
65	288	15	28.57	0.53	10.6±7.16
80	288	15	50	0.53	12.3±9.2
90	288	15	100	0.53	19.14±8.47

being continuously introduced into the PC by using high-pressure pump with pressure of 15 MPa. After reaching the temperature and pressure, subsequently, the LPM-PEG solution in MC was introduced into the PC. The CO_2 flow rate was fixed 3 kg/h, whereas the solution flow rate was fixed 0.53 mL/min. LPM concentration in the solution was fixed 10 mg/mL. Various PEG mass ratios were achieved by changing PEG concentration. Ratios mentioned here are referred to PEG mass ratios, to give easy understanding of the process, unless otherwise explained. After the entire solution was delivered to the PC, the co-precipitates were washed with CO_2 for 15 minutes to remove residual solvent. After depressurization, the co-precipitates on PTFE membrane filter were collected and analyzed. Summary of experimental condition and the result is given in Table 1.

3. Characterization

Morphology of co-precipitates was analyzed by using JEOL JSM-6700F scanning electron microscopy (SEM) (JEOL Ltd., Tokyo, Japan). Chemical distribution of particles was analyzed by elemental mapping, using SEM equipped with an energy dispersive X-ray spectroscope (EDS) (INCA Energy, Oxford Instruments, Abingdon, United Kingdom). The particle size and particle size distribution (PSD) were measured in the laser diffraction beam as an aerosolized dry powder using RODOS (Sympatec GmbH, Helos/BF, Clausthal-Zellerfeld, Germany) with dry powder accessory. Crystallinity was determined by powder X-ray diffraction (XRD) (D-Max-2500-C, Rigaku Co., Tokyo, Japan) analysis with Cu-Kα radiation. The diffraction patterns were measured with voltage of 50 kV and current of 200 mA in the 2θ angle range of 10° to 50° with 10°/min scanning rate. Drug-polymer interaction was analyzed by Fourier transform infrared (FT-IR) spectrophotometer (Nicolet 6700, Thermo Scientific, NJ, USA) in the wave number range from 650 to 4,000 cm^{-1}.

The LPM content in the co-precipitates was quantitatively determined with high performance liquid chromatography (HPLC) analysis. Sample solutions were prepared by dissolving 20 mg of co-precipitates in 10 ml methanol. The solution was diluted ten times with purified water and filtered through 0.5 μm PTFE membrane filter and analyzed by an Agilent 1200 HPLC-UV (Agilent Technology, USA) at λ=214 nm. The HPLC was equipped with auto-sampler and Eclipse XDB column (150×4 mm), which was packed with 5 μm C18. Chromatographic separations were performed using a mixture mobile phase of triethylamine hydrochloride buffer and acetonitrile (11 : 9 v/v) at a flow rate of 2 ml/min. The amount of injection was set at 50 μL and each sample was carried out in triplicate. In addition, the dissolution test of co-precipitates was conducted using a sample equivalent to 27 mg of LPM in 900 ml of 0.01 N HCl at 37±0.5 °C and 50 rpm paddle speed according to USP method 2 [18].

RESULTS AND DISCUSSION

Co-precipitates were analyzed by high performance liquid chromatography (HPLC) analysis to quantify the LPM content to ensure that the co-precipitates had similar LPM mass ratio with initial solution. Fig. 2 shows that similar ratio of the LPM content. This indicates that the LPM and PEG were well dispersed in the co-precipitates. In addition, scanning electron microscopy (SEM)-energy dispersive X-ray spectroscopy (EDS) analysis was conducted. Results of SEM analysis show that when 10-50% PEG mass ratios were used, the co-precipitates were in angular-shaped particles, which was similar to ASES-processed LPM. When 60-90% PEG mass ratios were used, the co-precipitates were in irregular-shaped particles, which was similar to ASES-processed PEG (Fig. 3). To ensure whether LPM and PEG were co-precipitated and well dispersed, EDS analysis was carried out [19,20] and the results are shown in Fig. 4. It revealed that chlorine and oxygen map overlapped each other. SEM, EDS, HPLC analysis indicated that LPM and PEG were co-precipitated particles and well dispersed.

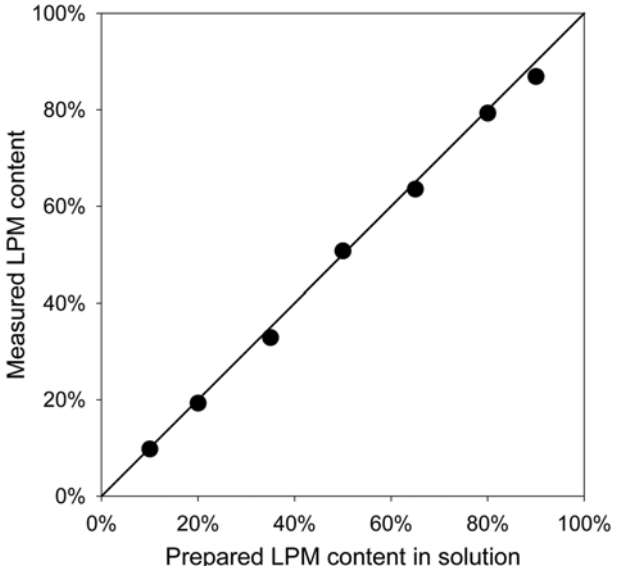

Fig. 2. Comparison of measured LPM content in the co-precipitates particles to its theoretical LPM content.

The co-precipitates were further characterized by determining size and distribution in various mass ratios of PEG that is shown in Fig. 5. At 10-50% PEG, the average particle size was less than 5 μm and no significant difference in its distribution. Significant different size occurred when the PEG mass ratio was more than 50%. Within those ratios, the average particle size was more than 10 μm and there was a broad particle size distribution. This might happen due to a stronger effect of crystal growth than the nucleation in the co-precipitates. Reverchon et al. [21] reported that higher solute concentration in solution can lead to higher supersaturation degree, produce many small nuclei at early stage and also increase the growth of the crystal. On the other hand, the higher PEG concentration in solution may result in increasing viscosity and stabilizing the liquid jet. Stabilized jet produces fewer droplets, which influences the area for mass transfer [22,23]. Combined with lower diffusion coefficient of solvent, high viscosity may result in low mass transfer and is likely to promote crystal growth than nucleation. Similar phenomena were observed in polymer precipitation using only polystyrene by Dixon et al. [22], only poly(l-lactic acid) by Randolph et al. [23], and copper-indomethachin by Warwick et al [24]. These reports suggest that higher PEG concentration in solution can promote crystal growth.

In addition, we determined co-precipitates crystallinity using powder X-ray diffraction (XRD). Fig. 6 shows XRD patterns of the raw materials (LPM and PEG) before ASES processing, after ASES

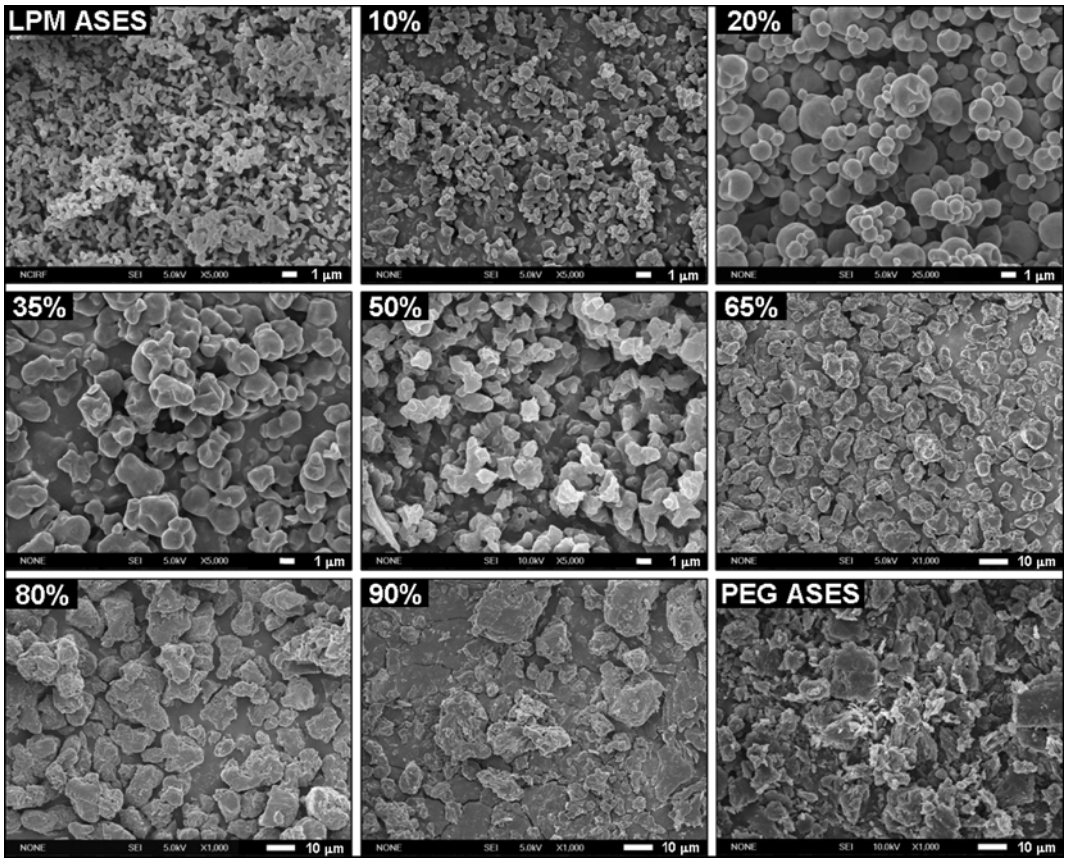

Fig. 3. SEM images of co-precipitates particle in various mass ratio of PEG.

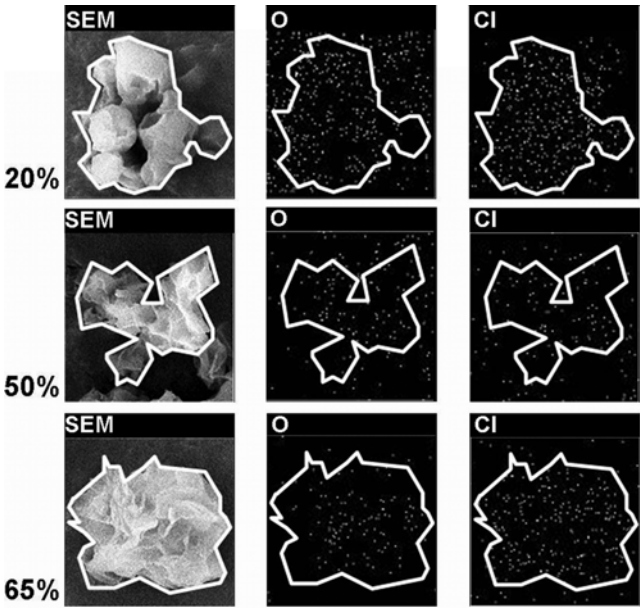

Fig. 4. SEM images with EDS analysis of (a) 20%, (b) 50%, and (c) 65% of PEG amount in the co-precipitates particles with its oxygen map (O) and its chlorine map (Cl).

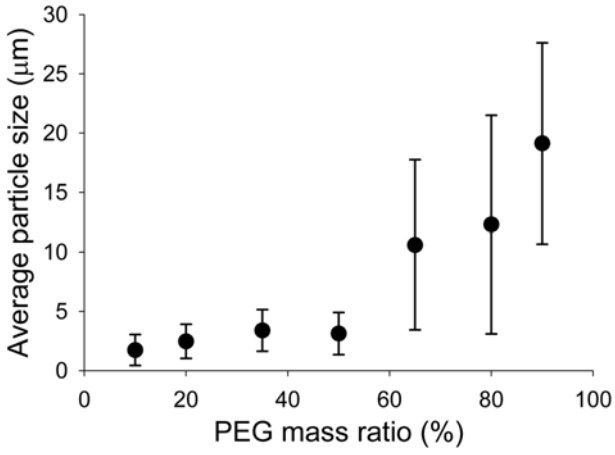

Fig. 5. Average particle size and particle size distribution of co-precipitation particles in various mass ratio of PEG.

processing and also co-precipitated particle in various mass ratios of PEG. The XRD patterns show sharp peak with high intensity for raw LPM at 16.7° and raw PEG at 19° and 23.1°, indicating that the raw LPM and PEG exhibited highly crystalline structure. After ASES-processing, the peak intensity decreased significantly in the pattern of LPM particles, whereas it remained the same in the pattern of PEG particles. The decreasing peak intensity of LPM particles after ASES-processed indicated amorphous form of LPM. It was observed that LPM is more easily precipitated than PEG during the ASES processing, which probably is due to the higher super saturation degree of LPM compared to that of PEG. Higher super saturation degree of LPM may result in formation of amorphous precipitate

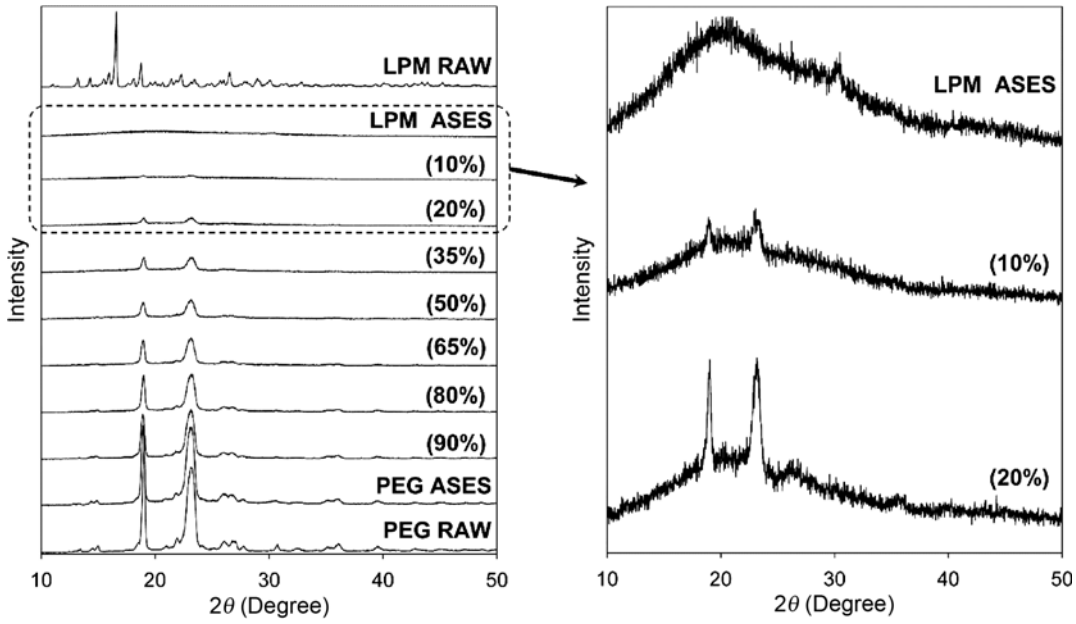

Fig. 6. XRD patterns of raw materials (LPM and PEG) before and after ASES processed, and co-precipitated particle in various mass ratio of PEG.

[25-27]. Amorphous form (loss of its crystalline structure) is commonly observed in ASES as reported by some authors [21,28-30]. The XRD patterns of co-precipitates in various mass ratios of PEG showed similar pattern with LPM ASES-processing and PEG ASES-processing. These patterns indicated that in the co-precipitates, the LPM was in the amorphous state, whereas the PEG was in the crystalline state. The intensity of crystalline PEG peak (19° and 23.1°) was reduced with reduced PEG content, indicating that more amorphous particles were produced with fewer polymers (PEG) amount. Based on XRD result, the co-precipitates structure was LPM, amorphous drug entrapped between semi-crystalline structures of PEG (interstitial solid solution). This structure was formed due to the crystalline nature of PEG, which determined the end structure of the co-precipitate [1].

LPM-PEG interaction was further analyzed by Fourier transform infrared (FT-IR) spectrophotometry, a powerful method for analyzing intermolecular and intramolecular forces. By careful examination of each stretching region, structure and molecular interaction with the co-precipitates can be determined as shift of peak maxima [31]. Fig. 7 shows that the maxima of carbonyl (-C(O)-N=) stretching (1,620 cm^{-1}) observed in the LPM raw material was shifted to a higher

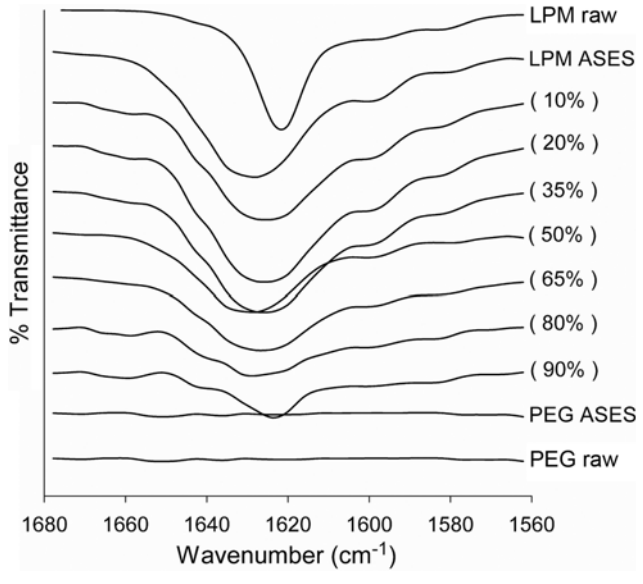

Fig. 7. FT-IR spectra of raw materials (LPM and PEG) before and after ASES processed, and co-precipitated particle in various mass ratio of PEG showing carbonyl stretching region.

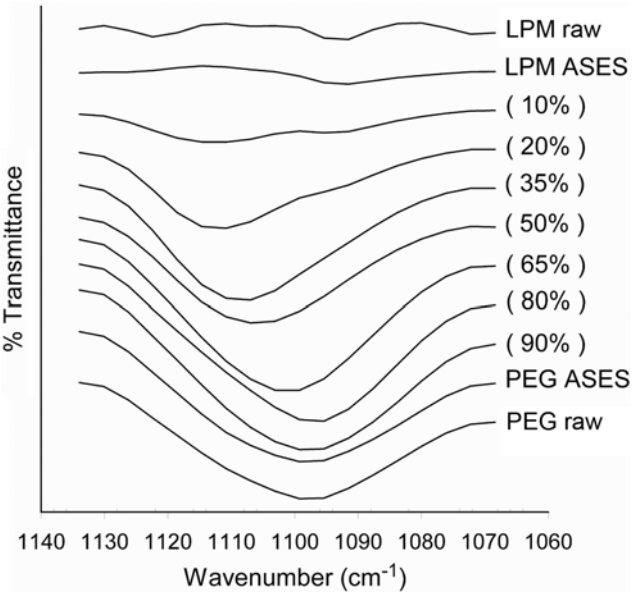

Fig. 8. FT-IR spectra of raw materials (LPM and PEG) before and after ASES processed, and co-precipitated particle in various mass ratio of PEG showing ether stretching region.

wavenumber (1,624-1,628 cm^{-1}) for LPM ASES-processed and the co-precipitates in various mass ratio of PEG. The shift of this peak was probably due to the change of LPM structure from crystalline form (hydrogen bonded to carbonyl) to amorphous form (no-hydrogen bonded to carbonyl) [31].

Ether bond (-C-O-C) in ethylene glycol can interact with another bond and can be recognized by peak maxima shift. Fig. 8 shows stretch peaks of ether at 1,106-1,111 cm^{-1} in the FT-IR spectra of PEG raw material, PEG ASES-processed and the co-precipitates in various mass ratio of PEG. In FT-IR of PEG raw material, PEG ASES-processed and the co-precipitates with 65-90% PEG mass ratios, stretch peak of ether was maximum at 1,099 cm^{-1} whereas the maximum peak of the co-precipitates with 10-50% PEG mass ratios was at 1,106-1,111 cm^{-1}. The shift of this peak was not caused by the change of ether bond as its stretching peak will shift to lower number because of interaction as found in multiwall carbon nanotubes [32] or dye-sensitized solar cells [33]. The peak maxima shift might be related to the morphology change in PEG (see Fig. 3). In 65-90% PEG mass ratios, all the LPM was entrapped in the interstitial volume of stacked PEG due to high amount of PEG present. At that point, the PEG chain was fully stretched and stacked as multilayered structure and had irregular crystalline morphology. In 10-50% PEG mass ratios, interstitial volume did not provide enough volume to entrap all the LPM. Since the PEG has an ability to fold [34,35], PEG folded and formed more random structure to encapsulate the LPM, resulting in a loss of crystal morphology and became angular-shaped particles, which was similar to LPM ASES-processed. Thus, the shift of ether stretch peaks might indicate a sign of PEG chain folding. Although all FT-IR spectra showed no interaction between LPM and PEG, bond and intermolecular interaction was needed to keep those molecules attached. Thus, it was suggested that co-precipitates involved non specific interaction such as van der Waals, which could not be detected by FT-IR [32].

The performance of co-precipitates was further studied using dissolution. Fig. 9 shows the dissolution profile of the co-precipitates with 50% PEG mass ratio compare to raw LPM (size: 34.93±31.88 μm) and LPM ASES-processed (size: 1.64±1.34 μm). LPM ASES-processed had higher dissolution rate compared to raw LPM at 5 to 20 minutes. It is because LPM ASES-processed was in amorphous form so it had higher energy level, which increased dissolution rate [4,36]. On the other hand, rapid dissolution of LPM ASES-processed induced interparticle bridge during dissolution and caused agglomeration. Therefore, the dissolution of LPM ASES-processed was slower than raw LPM after 20 minutes. A significant enhancement in dissolution rate was observed in co-precipitates. In co-precipitates, LPM was co-precipitated in amorphous form and PEG acted as wetting agent. As a result, agglomeration was hindered and faster dissolution rate of co-precipitates compared to that of raw LPM and LPM ASES-processed was achieved.

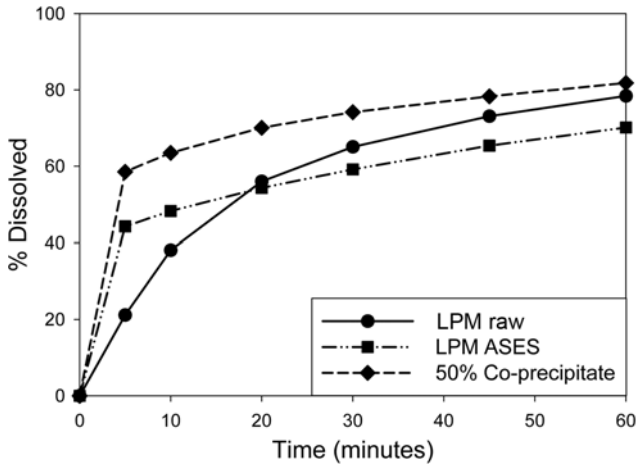

Fig. 9. Dissolution profile of co-precipitated particle with 50% PEG mass ratio compare to LPM before and after ASES processed.

CONCLUSION

The co-precipitation of loperamide hydrochloride (LPM) and polyethylene glycol (PEG) using aerosol solvent extraction system (ASES) in various mass ratios of PEG resulted in amorphous structure of LPM and crystalline structure of PEG. The particle shape was determined such that in 10-50% PEG mass ratios, angular-shape was formed, whereas in 65-90% PEG mass ratios, irregular-shape was formed. LPM was well-dispersed in PEG as a polymer and the co-precipitates showed better dissolution rate compared to LPM before and after ASES-processing.

ACKNOWLEDGEMENT

This research was partially supported by PT Dexa Medica, Indonesia. We thank Audrey Clarissa and Sherly Juliani for careful reading of this manuscript.

LIST OF ABBREVIATION

LPM : loperamide hydrochloride
PEG : polyethylene glycol
ASES : aerosol solvent extraction system
SEM : scanning electron microscope
EDS : dispersive X-ray spectroscopy
XRD : X-ray diffraction
FT-IR : fourier transform infra red
BCS : biopharmaceutics classification system
HPLC : high pressure liquid chromatography
MC : methylene chloride

REFERENCES

1. J. Kluge, F. Fusaro, G. Muhrer, R. Thakur and M. Mazzotti, *J. Supercrit. Fluids*, **48**, 176 (2009).
2. C. Leuner and J. Dressman, *Eur. J. Pharm. Biopharm.*, **50**, 47 (2000).
3. M. P. Patil and N. J. Gaikwad, *Acta Pharm.*, **59**, 57 (2009).
4. A. T. M. Serajuddin, *J. Pharm. Sci.*, **88**, 1058 (1999).
5. H. Liu, L.-L. Zhou, L.-L. Wei, H. Guo, S.-F. Nie, X.-G. Yang, R. Tang and W.-S. Pan, *Drug Dev. Ind. Pharm.*, **33**, 959 (2007).
6. I. Pasqualli and R. Bettini, *Int. J. Pharmceut.*, **364**, 176 (2008).
7. Y.-S. Youn, J. H. Oh, K. H. Ahn, M. Kim, J. Kim and Y.-W. Lee, *J. Supercrit. Fluids*, **59**, 117 (2011).
8. J. Chu, G. Li, K. H. Row, H. Kim and Y.-W. Lee, *Int. J. Pharm.*, **369**, 85 (2009).

9. J. Chu, H. Lee, H. Kim and Y.-W. Lee, *Korean J. Chem. Eng*., **26**, 1119 (2009).
10. C.-W. Lee, S.-J. Kim, Y.-S. Youn, E. Widjojokusumo, Y.-H. Lee, J. Kim and Y.-W. Lee, *J. Supercrit. Fluids*, **55**, 348 (2010).
11. M. Türk, G. Upper, M. Steurenthaler, Kh. Hussein and M. A. Wahl, *J. Supercrit. Fluids*, **39**, 435 (2007).
12. J. Jung and M. Perrut, *J. Supercrit. Fluids*, **20**, 179 (2001).
13. E. Badens, V. Majerik, G. Horváth, L. Szokonya, N. Bosc, E. Teillaud and G. Charbitb, *Int. J. Pharm*., **377**, 25 (2009).
14. A. Martin, F. Mattea, L. Gutierrez, F. Miguel and M. J. Cocerro, *J. Supercrit. Fluids*, **41**, 138 (2007).
15. O. I. Corrigan and A. M. Crean, *Int. J. Pharm*., **245**, 75 (2002).
16. S. Sethia and E. Squillante, *Int. J. Pharm*., **272**, 1 (2004).
17. G. Muhrer, U. Meier, F. Fusaro, S. Albano and M. Mazzotti, *Int. J. Pharm*., **308**, 69 (2006).
18. *Loperamide hydrochloride tablets*, **USP32-NF27**, 2802 (2008).
19. E. Reverchon and A. Antonacci, *Biotechnol. Bioeng*., **97**, 1626 (2007).
20. E. Reverchon, G. Lamberti and A. Antonacci, *J. Supercrit. Fluids*, **4**, 185 (2008).
21. E. Reverchon, I. De Marco and E. Torino, *J. Supercrit. Fluids*, **43**, 126 (2007).
22. D. J. Dixon, P. Johnston and R. A. Bodmeir, *AIChE J.*, **39**, 127 (1993).
23. T. W. Randolph, A. D. Randolph, M. Mebes and S. Yeung, *Biotechnol. Prog*., **9**, 429 (1993).
24. B. Warwick, F. Dehghani, N. R. Foster, J. R. Biffin and H. L. Regtop, *Ind. Eng. Chem. Res*., **41**, 1993 (2002).
25. M. E. Matteuci, M. A. Miller, R. O. Williams III and K. P. Johnston, *J. Phys. Chem. B*., **112**, 16675 (2008).
26. M. E. Matteuci, J. Paguio, M. Miller, R. Williams III and K. Johnston, *Pharm. Res*., **25**, 2477 (2008).
27. M. E. Matteucci, B. K. Brettmann, T. L. Rogers, E. J. Elder, R. O. Williams III and K. P. Johnston, *Mol. Pharm*., **4**, 182 (2007).
28. E. Reverchon and G. Della Porta, *Powder Technol*., **106**, 23 (1999).
29. A. Tenorio, M. D. Gordillo, C. Pereyra and E. J. Martínez de la Ossa, *J. Supercrit. Fluids*, **40**, 308 (2008).
30. M. A. Tavares Cordoso, V. Geraldes, J. M. S. Cabral and A. M. F. Palavra, *J. Supercrit. Fluids*, **46**, 71 (2008).
31. H. Konno and L. S. Taylor, *J. Pharm. Sci*., **95**, 2692 (2006).
32. S. Kubota, T. Maruyama, H. Nishikiori, N. Tanaka, M. Endo and T. Fujii, *Chem. Lett*., **38**, 890 (2009).
33. M.-S. Kang, J. H. Kim, J. Won and Y. S. Kang, *J. Photochem. Photobiol. A*., **183**, 15 (2006).
34. D. Q. M. Craig and J. M. Newton, *Int. J. Pharm*., **74**, 33 (1991).
35. C. P. Buckley and A. J. Kovacs, *Colloid Polym. Sci*., **254**, 695 (1976).
36. D. Q. M. Craig, *Int. J Pharm*., **231**, 131 (2002).